Composite Structures 122 (2015) 82–91

Contents lists available at ScienceDirect

Composite Structures

journal homepage: www.elsevier.com/locate/compstruct

Effect of initial tool-plate curvature on snap-through load of unsymmetric laminated cross-ply bistable composites

Jong-Gu Lee [a], Junghyun Ryu [a], Seung-Won Kim [b], Je-Sung Koh [b], Kyu-Jin Cho [b], Maenghyo Cho [a,*]

[a] Smart Structures & Design Laboratory, School of Mechanical and Aerospace Engineering/IAMD, Seoul National University, Gwanak 599 Gwanak-ro, Gwanak-gu, Seoul 151-742, Republic of Korea

[b] Biorobotics Laboratory, School of Mechanical and Aerospace Engineering/IAMD, Seoul National University, Gwanak 599 Gwanak-ro, Gwanak-gu, Seoul 151-742, Republic of Korea

ARTICLE INFO

Article history:
Available online 21 November 2014

Keywords:
Bistable composite
Snap-through
Residual stress
Initial curvature

ABSTRACT

In this study, the effect of the initial curvature of a tool plate on the snap-through load of square cross-ply bistable composites was analyzed. The snap-through load is a function of the cured curvature and residual moment. In the curing process, both these physical quantities are affected by the initial tool-plate curvature. As a result, the snap-through load can also be changed by adjusting the initial tool-plate curvature. Then, for evaluating its effect on the snap-through load, a snap-through process was simulated by minimizing the total potential energy of the bistable composites through the Rayleigh–Ritz approximation method. The simulation results show that the snap-through load changes linearly with the initial tool-plate curvature. The simulation results are compared with those obtained experimentally and by a finite element analysis (FEA) in order to verify the pre-identified effect of the initial tool-plate curvature.

1. Introduction

Bistable composites have two stable shape (cylindrical shapes [1–7] or saddle shapes [8]) as a result of the coupling effect between their residual stress and geometric nonlinearity. These composites can be snapped through (i.e. from one stable shape to the other at a specific mechanical load) [9–11]. During this snap-through action, a large out-of-plane deflection occurs at a fast time scale with respect to quasi-static phenomena. After snap-through, the bistable composites remain in a stable state without requiring any additional energy supply to maintain a constant shape. Owing to these interesting properties, bistable composites have attracted research attention in the fields of aerodynamics, energy harvesting and robotics for developing a high-energy-efficiency morphing structure or device [12–21].

In the field of aerodynamics, the concept of a morphing airfoil was proposed on the basis of bistable composites [12–16]. Furthermore, analytical models were developed to design and control the morphing airfoil based on bi-stable composites [17,18]. Further, in the field of energy harvesting, an energy harvesting device was first developed by combining bistable composite plates with a piezoelectric patch for effective energy harvesting and subsequently analyzed [19,20]. In the field of biomimetics, a flytrap-inspired robot was developed by employing a cross-ply laminated bistable composite. This robot was found to well mimic the prey capture behavior of the Venus flytrap owing to the snap-through action of the bistable composite [21].

Generally, morphing structures such as a morphing wing or a flytrap-inspired robot require different stable shapes and different structural stabilities depending on the circumstances (e.g., the flight condition or the open and closed states of a flytrap) [13,17]. For this reason, the cured curvatures or the snap-through load of bistable composites should be adjusted differently in each stable state depending on the design requirement.

Unfortunately, this adjustment is not easy to perform, because unsymmetric cross-ply laminates are ordinarily cured on a flat tool plate. Moreover, if the laminates have an alternating layers of orthotropic laminae with equal thickness and identical material properties on both sides of the mid-plane axis, e.g., [90°/0°], [90°/0°/90°/0°], or [90°/90°/0°/0°], the cured curvatures of both the stable states are forced to be identical to each other, and so are the snap-through loads of these states.

Although the desired result is expected to be obtained by the modification of the lay-up sequence of laminates, e.g., [90°/90°/90°/0°/0°], this approach results in alteration of other design-dependent variables (e.g., the thickness and stiffness of laminates). As a result, this design approach of bistable composites results in a structurally overweight or a mechanically over-stiff composite. Therefore, to be able to apply the design of bistable

* Corresponding author. Tel.: +82 2 880 1693; fax: +82 2 886 1645.
E-mail address: mhcho@snu.ac.kr (M. Cho).

http://dx.doi.org/10.1016/j.compstruct.2014.11.037
0263-8223/

composites more flexibly to morphing structures, it would be desirable to consider a method for adjusting the cured curvature or the snap-through load while minimizing the change in the design-dependent variables.

Several strategies were introduced to address this problem. These can be categorized into three strategies. One strategy is to connect the different angle-ply laminated composites with each other in parallel or series [22–24]. From this strategy, the multi-stable shape of bi-stable composite was attained and controlled without changing the thickness of composite. Another strategy is to prestress the selected plies of symmetric laminates before curing process by means of the specifically manufactured prestress machine [25,26]. The snap-through load and curvature of the symmetric laminated composites was tailored by unsymmetrically prestressing on the basis of the neutral axis. Other approach is to apply an initial curvature to unsymmetric laminated composites by using an initially curved tool plate [5,27]. In this approach, the initial curvature of the tool plate affects the cured curvature while keeping the thickness and stiffness of the composites.

Although the previous paper [5,27] did not focus on the snap-through load, it is an important design factor in the practical application of morphing structures that are based on the snap-through action of bistable composites. Accordingly, in addition to curvature tailoring, the snap-through load of bistable composites also needs to be adjusted.

On the basis of the logic explained below, we expect that the snap-through load can be adjusted by tailoring the initial tool-plate curvature. The initial tool-plate curvature affects the cured curvature; this cured curvature is closely related to the bending deformation energy of the bistable composite, which is required to be supplied until a snap-through occurs. Consequently, because the snap-through load is also related to the bending deformation energy, this load will also be affected by a change in the cured curvature induced by a change in the initial tool-plate curvature.

If the effect of the initial tool-plate curvature on the snap-through load can be evaluated, the snap-through load of bistable composites could also be adjusted to meet various design requirements. Then, it would be possible to effectively apply bistable composites as morphing structures, which require different structural shapes and different structural stabilities depending on the circumstances. The present study therefore aims to estimate the effect of the initial tool-plate curvature on the snap-through load of unsymmetric cross-ply laminated composites. First, a snap-through process is simulated by minimizing the total potential energy of the square cross-ply bistable composites, by employing the Rayleigh–Ritz approximation method. The simulation results show that the snap-through load changes linearly with the initial tool-plate curvature. These results are compared with those obtained experimentally and by a finite element analysis (FEA) in order to validate the pre-identified effect of the initial tool-plate curvature on the snap-through load.

2. Snap-through of bistable composite and its driving mechanism

Two stable shapes of the square cross-ply bistable composite are defined as Mode 1 and Mode 2 depending on the orientation of the curvature of the bistable composite with respect to the initial tool-plate curvature, as illustrated in Fig. 1. Specifically, Mode 1 is defined as a cylindrical shape in which the dominant curvature is parallel to the initial tool-plate curvature, i.e., the x-directional curvature κ_{xx}. On the other hand, Mode 2 is defined as a cylindrical shape in which the dominant curvature is perpendicular to the initial tool-plate curvature, i.e., the y-directional curvature κ_{yy}.

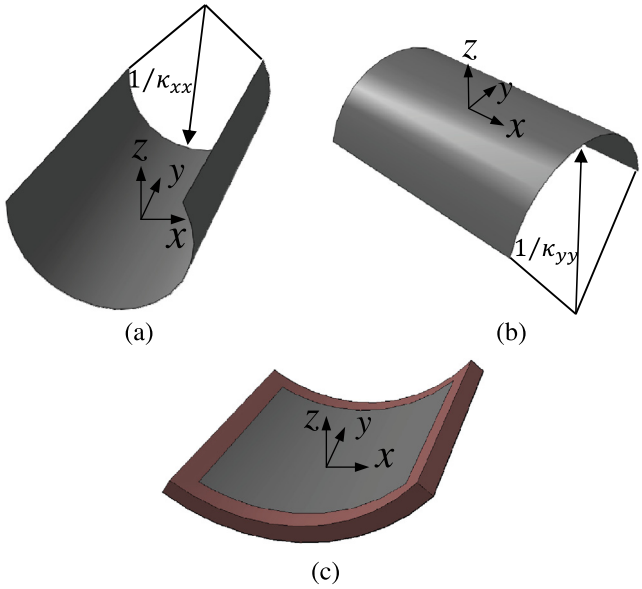

Fig. 1. Two stable configurations of square cross-ply bistable composites: (a) Mode 1: $\kappa_{xx} > 0$, $\kappa_{yy} \approx 0$; (b) Mode 2: $\kappa_{xx} \approx 0$, $\kappa_{yy} < 0$; and (c) tool plate: $\kappa_{xx} \neq 0$, $\kappa_{yy} = 0$.

The snap-through process is separately categorized into a snap-forth process and a snap-back process depending on the sequence of mode change. Specifically, snap-forth refers to snap-through from Mode 1 to Mode 2, and snap-back refers to snap-through from Mode 2 to Mode 1, as illustrated in Fig. 2.

In order to induce snap-through, a mechanical load should be applied with the aim of unrolling the bistable composite. For example, if an x-directional moment is applied to the bistable composite in Mode 1, it will just unroll while maintaining the x-directionally curved cylindrical shape at the beginning of deformation. However, when the dominant curvature of the bistable composite reaches a certain x-directional deformation curvature (henceforth referred to as the "snap-forth starting curvature"), the composite starts transforming from Mode 1 to Mode 2 (i.e., snap-forth) by itself. In other words, at the snap-forth starting curvature, the direction of the dominant curvature starts changing from the x-direction to the y-direction, which is perpendicular to the direction of the external moment and direction of the dominant curvature.

In order to explain the above phenomenon, we make the following two assumptions:

1. A driving mechanism exists that is acting perpendicular to the direction of the dominant curvature of each mode.
2. The snap-through starting curvature is the minimum or critical curvature at which the driving mechanism is sustained.

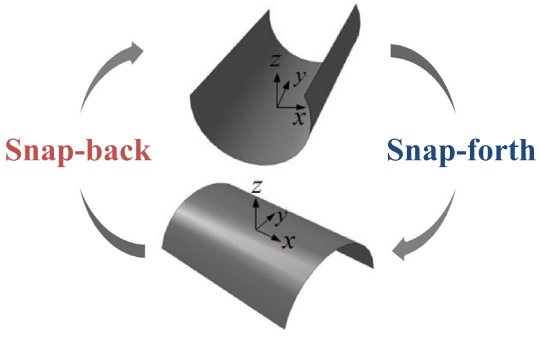

Fig. 2. Schematic of snap-forth and snap-back processes.

In fact, in the case of Mode 1, the internal residual moment is induced in the y-direction, which is perpendicular to the direction of the dominant curvature. This y-directional internal residual moment ($_{Mode\ 1}M_y^{residual}$) is distributed along the x-directional edge, as shown in Fig. 3. The internal residual moment becomes zero at the free edge ($y = \pm L/2$) in order to satisfy the stress-free boundary condition. However, it rapidly recovers to a constant value when it approaches the interior region of the cylindrical panel. In this study, we focus only on the constant internal residual moment away from the free edges.

The constant internal residual moment (hereafter simply called "residual moment") acts in a direction perpendicular to the direction of the dominant curvature of each mode. Therefore, this residual moment might be one of the important factors that trigger the snap-through mechanism. Consequently, the snap-forth starting curvature mentioned in the second assumption above can be reinterpreted as being the minimum curvature at which the residual moment can be sustained. According to the second assumption, the snap-forth load would also be affected by the change in the snap-forth starting curvature with a change in the y-directional residual moment. Contrary to the case of snap-forth, in the case of snap-back, the snap-back load would be affected by the x-directional residual moment.

Therefore, the residual moment, in addition to the cured curvature, is an important factor in the design of the snap-through load. For example, in the prediction of the snap-forth load, both the x-directional cured curvature and the y-directional residual moment should be considered. Similarly, in the prediction of the snap-back load, both the y-directional cured curvature and the x-directional residual moment should be considered.

For these reasons, changes in the residual moment and cured curvature with the initial tool-plate curvature need to be examined prior to predicting the change in the snap-through load induced by the initial tool-plate curvature. First, the cured curvature, as well as the mid-plane strain fields, can be easily estimated by using the explicit model of Ryu et al. [27]. Next, the residual moment can be estimated from the definition of moment resultant in the classical laminate theory. The material properties and stacking sequence of the laminated composites were adopted from the study of Ryu et al. [27].

As an example, the cured curvature and residual moment were estimated under increasing x-directional initial tool-plate curvature. When the bistable composite is in Mode 1, the x-directional initial tool-plate curvature affects only the x-directional cured curvature of Mode 1, as shown in Fig. 4(a). However, when the bistable composite is in Mode 2, the x-directional initial tool-plate curvature affects only the x-directional residual moment of Mode 2, as shown in Fig. 4(b). In addition, both quantities (i.e. the x-directional cured curvature of Mode 1 and the x-directional residual moment of Mode 2) are increased with increasing initial curvature.

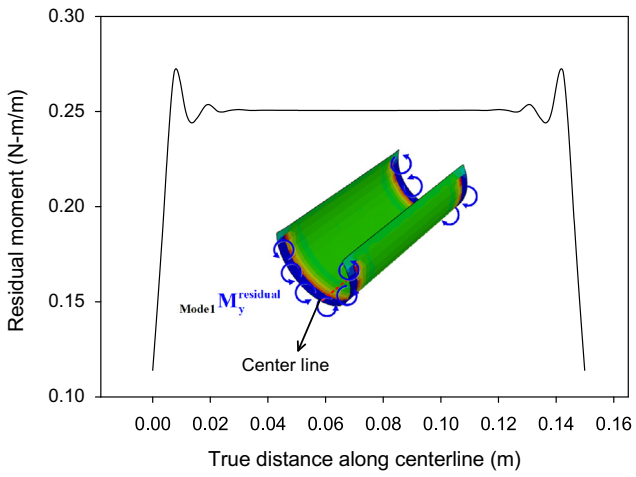

Fig. 3. Distribution of internal residual moment along centerline of bistable composites (FEA result of unsymmetrically laminated cross-ply bistable composite).

If the two abovementioned assumptions are correct and when the abovementioned known relation between the cured curvature and the x-directional initial tool-plate curvature is considered, application of the x-directional initial tool-plate curvature will have the following effects.

1. In the case of snap-forth, the snap-through starting curvature should not be changed, because the y-directional residual moment of Mode 1, which is the driving mechanism for the snap-forth process, is not affected by the x-directional initial tool-plate curvature.
2. In the case of snap-back, the snap-through starting curvature should be increased because the x-directional residual moment of Mode 2, which is the driving mechanism for the snap-back process, increases with increasing x-directional initial tool-plate curvature.
3. Considering the two assumptions and the known relation between the cured curvature and the x-directional initial tool-plate curvature, the snap-forth load should be increased with increasing the x-directional initial tool-plate curvature. In contrast to the snap-forth load, the snap-back load should be decreased with increasing the x-directional initial tool-plate curvature.

3. Snap-through of bistable composites subjected to line-edge moment

In this section, we estimate the snap-forth and snap-back loads (moments) by the Rayleigh–Ritz approximation method to determine the relationship between the snap-through load and the initial tool-plate curvature.

3.1. Simple analytical model

The simple analytical model is derived by minimizing the total potential energy including a moment equilibrium condition. The minimization is performed using the Rayleigh–Ritz approximation method as follows:

$$\delta\Pi^* = \delta\Pi + \delta\left\{\Lambda\left(\int_{-\frac{L}{2}}^{\frac{L}{2}} M^{external}dl - \int_{-\frac{L}{2}}^{\frac{L}{2}} M^{internal}dl\right)\right\} \tag{1}$$

where $\delta\Pi^*$ is the first variation of the total potential energy and $\delta\Pi$ is the first variation of the strain energy of the bistable composite. The difference between the internal moment $M^{internal}$ and the external moment $M^{external}$ acts as the moment equilibrium constraint that conjugates to the Lagrange multiplier Λ.

3.1.1. Strain energy of bistable composites

Assuming a plane stress state, the strain energy of unsymmetric cross-ply laminated composites with initial tool-plate curvature is expressed as

$$\Pi = \sum_{i=1}^{n}\int_{-\frac{L}{2}}^{\frac{L}{2}}\int_{-\frac{L}{2}}^{\frac{L}{2}}\int_{z_i^{low}}^{z_i^{up}} \frac{1}{2}\overline{Q}_{11}^i\varepsilon_{xx}^2 + \frac{1}{2}\overline{Q}_{22}^i\varepsilon_{yy}^2 + \overline{Q}_{12}^i\varepsilon_{xx}\varepsilon_{yy} + \frac{1}{2}\overline{Q}_{66}^i\gamma_{xy}^2 dzdxdy \tag{2}$$

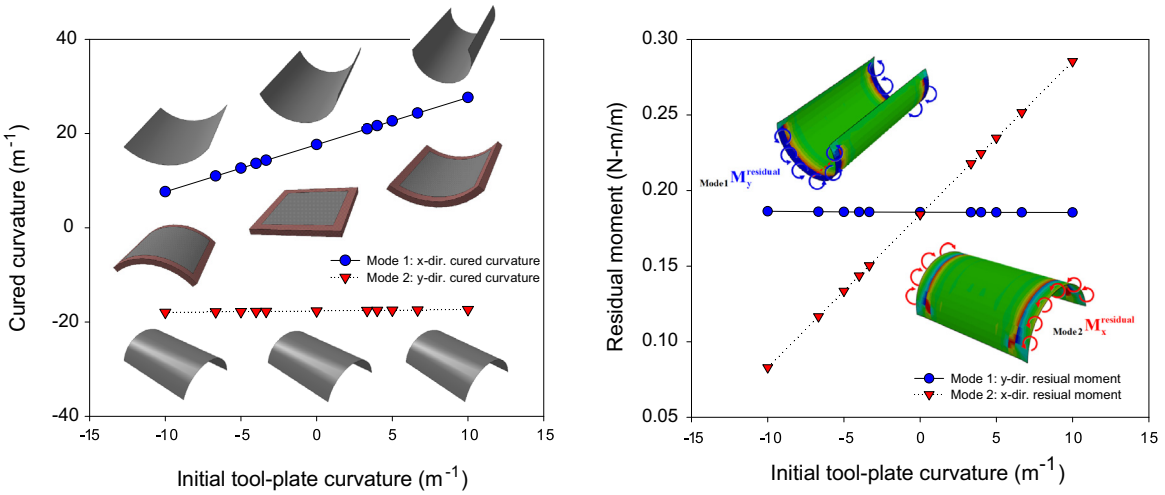

Fig. 4. Cured curvature and residual moment as a function of x-directional initial tool-plate curvature (analysis results).

where $\overline{Q}^{i}_{\alpha\beta}$ is the transformed plane-stress reduced stiffness of the ith layer; L is the side length of the composites; and z_i^{up} and z_i^{low} denote the positions of the upper surface and lower surface, respectively, corresponding to the ith layer. The elastic strains $\varepsilon_{xx}, \varepsilon_{yy}, \gamma_{xy}$ are given by the difference between the total strains and the inelastic strains, as expressed in Eq. (3):

$$\begin{Bmatrix} \varepsilon_{xx} \\ \varepsilon_{yy} \\ \gamma_{xy} \end{Bmatrix} = \begin{Bmatrix} \varepsilon_{xx}^{total} \\ \varepsilon_{yy}^{total} \\ \gamma_{xy}^{total} \end{Bmatrix} - \begin{Bmatrix} \varepsilon_{xx}^{inelastic} \\ \varepsilon_{yy}^{inelastic} \\ \gamma_{xy}^{inelastic} \end{Bmatrix} = \left\{ \begin{bmatrix} \xi_{xx} + \lambda_{xx} y^2 \\ \xi_{yy} + \lambda_{yy} x^2 \\ (\kappa_{xx}\kappa_{yy} + 2\lambda_{xx} + 2\lambda_{yy}) xy \end{bmatrix} + \begin{bmatrix} -\kappa_{xx} \\ -\kappa_{yy} \\ 0 \end{bmatrix} z \right\} - \left\{ \begin{bmatrix} \alpha_{xx}\Delta T \\ \alpha_{yy}\Delta T \\ \alpha_{xy}\Delta T \end{bmatrix} + \begin{bmatrix} \kappa_{xx}^{initial} \\ 0 \\ 0 \end{bmatrix} z \right\} \tag{3}$$

Inelastic strains are defined as the sum of the thermal strains and the strain induced by the initial tool-plate curvature. Thermal strains are defined as the product of the thermal coefficients $\alpha_{xx}, \alpha_{yy}, \alpha_{xy}$ and the change in temperature, ΔT. The tool-plate-induced strains are expressed as the product of the initial tool-plate curvature $\kappa_{xx}^{initial}$ and the distance from the mid-plane axis, z. The total strains $\varepsilon_{xx}^{total}, \varepsilon_{yy}^{total}, \gamma_{xy}^{total}$ are represented by a quadratic form that has six undetermined Ritz coefficients: the constant mid-plane strain terms ξ_{xx}, ξ_{yy}, the quadratic mid-plane strain terms $\lambda_{xx}, \lambda_{yy}$, and the constant curvatures κ_{xx}, κ_{yy} of the bistable composite. The total strains are derived by making three assumptions—assumption of an infinitesimal strain, assumption of a Kirchhoff–Love thin plate/shell, and assumption of a constant curvature shape [27].

3.1.2. Moment equilibrium

The internal and external moments must be compared to determine whether or not the moment equilibrium condition has been satisfied. For this comparison, the internal moment should be calculated by considering the neutral axis.

Generally, the moment resultant is defined on the basis of the mid-plane axis in the classical laminate theory. However, in the case of unsymmetric cross-ply laminated composites, the mid-plane axis does not coincide with the neutral axis. Therefore, the internal moment resultant should be recalculated on the basis of the neutral axis.

In the case of snap-forth, since the external moment is applied along the edge (i.e., $x = \pm L/2$), the corresponding internal moment is recalculated as follows:

$$\int_{-\frac{L}{2}}^{\frac{L}{2}} M_x^{internal} \mathrm{d}y = \left(\sum_{i=1}^{n} \int_{-\frac{L}{2}}^{\frac{L}{2}} \int_{z_i^{low}}^{z_i^{top}} (Q_{11}^i \varepsilon_{11} + Q_{12}^i \varepsilon_{22})(z-d) dz dy \right) \Bigg|_{x=\pm\frac{L}{2}} \tag{4}$$

where d is the distance from the mid-plane axis to the neutral axis, as illustrated in Fig. 5.

Further, in the case of snap-back, since the external moment is applied to the edge (i.e., $y = \pm L/2$), the corresponding internal moment is recalculated as

$$\int_{-\frac{L}{2}}^{\frac{L}{2}} M_y^{internal} \mathrm{d}x = \left(\sum_{i=1}^{n} \int_{-\frac{L}{2}}^{\frac{L}{2}} \int_{z_i^{low}}^{z_{itop}} (Q_{21}^i \varepsilon_{11} + Q_{22}^i \varepsilon_{22})(z+d) dz dx \right) \Bigg|_{y=\pm\frac{L}{2}} \tag{5}$$

3.1.3. Minimization of total potential energy

The first variation of the total potential energy, $\delta\Pi^*$, should be equal to zero to ensure the existence of a solution. The requirement for the existence of a solution is given as follows:

$$\delta\Pi^* = \left(\frac{\partial\Pi^*}{\partial\xi_{xx}}\right)\delta\xi_{xx} + \left(\frac{\partial\Pi^*}{\partial\xi_{yy}}\right)\delta\xi_{yy} + \left(\frac{\partial\Pi^*}{\partial\lambda_{xx}}\right)\delta\lambda_{xx} + \left(\frac{\partial\Pi^*}{\partial\lambda_{yy}}\right)\delta\lambda_{yy} + \left(\frac{\partial\Pi^*}{\partial\kappa_{xx}}\right)\delta\kappa_{xx} + \left(\frac{\partial\Pi^*}{\partial\kappa_{yy}}\right)\delta\kappa_{yy} + \left(\frac{\partial\Pi^*}{\partial\Lambda}\right)\delta\Lambda = 0 \tag{6}$$

Eq. (6) is a compilation of nonlinear algebraic equations that have seven unknowns: $\xi_{xx}, \xi_{yy}, \lambda_{xx}, \lambda_{yy}, \kappa_{xx}, \kappa_{yy}, \Lambda$. In order to solve these nonlinear algebraic equations, the Newton–Raphson iterative method is used. The cylindrical shape of Mode 1 for snap-forth and the cylindrical shape of Mode 2 for snap-back is assumed as an initial solution. In each subsequent step (i.e., loading step), an initial solution uses the calculation result obtained in the previous step.

3.2. Analysis results

Cross-ply [0/90] bistable composites with x-directional initial tool-plate curvatures of 0, 4, 5, 6.66, and 8.33 m^{-1} are considered in this study. Properties of the material of the lamina, i.e., carbon fiber prepreg, are summarized in Table 1; these properties are also

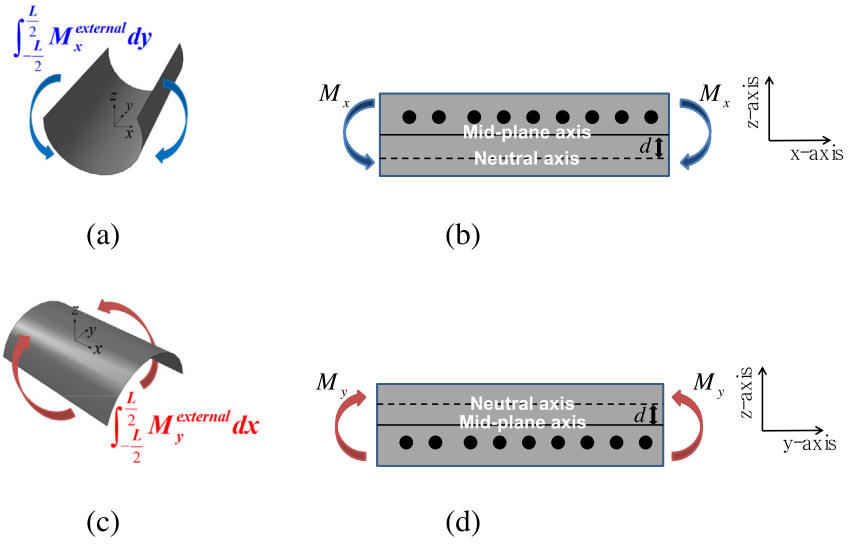

Fig. 5. Schematics of loading conditions and positions of neutral axes: (a) and (b) snap-forth and (c) and (d) snap-back.

Table 1
Material properties of carbon fiber prepreg.

Parameter		Unit	
Axial tensile modulus	E_1	GPa	96
Transversal tensile modulus	E_2	GPa	6.9
Shear modulus	G_{12}	GPa	3.4
Poisson's ratio	ν_{12}		0.3
Thickness	t	mm	0.085
Thermal expansion coefficient parallel to fiber direction	α_1	°C^{-1}	0.19e^{-6}
Thermal expansion coefficient perpendicular to fiber direction	α_2	°C^{-1}	38e^{-6}
Temperature change	ΔT	°C	−145

considered in the experiments described later in the paper. The lamina material used in the study is CU 0503 carbon fiber reinforced plastic (Hankuk Carbon). The prepreg is cut into squares with a side length of 150 mm.

In the snap-through analysis, the moment is applied along the edge (i.e., $x = \pm L/2$ for snap-forth and $y = \pm L/2$ for snap-back), as illustrated in Fig. 5. During the application of the moment, the deformation curvatures are estimated at regular intervals. The snap-through moment is the value at which the strain energy of the bistable composites attains a maximum.

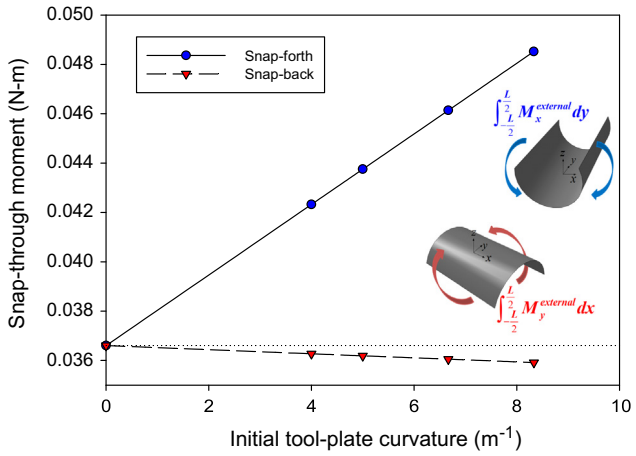

Fig. 6. Change in snap-through moment with initial tool-plate curvature (analysis results).

As is clear from the results of the snap-through analysis shown in Fig. 6, the snap-forth moment increases linearly with the initial tool-plate curvature. However, the snap-back moment decreases linearly with increasing initial tool-plate curvature.

The snap-through moment can be predicted easily but quite accurately if the cured curvature and snap-through starting curvature are both known. This is because the bending rigidity of the bistable composite is nearly constant before the snap-through process starts but it decreases rapidly after snap-through occurs, as shown in Fig. 7. As a result, the snap-through moment can be approximated as a product of the bending rigidity and the difference between the cured curvature and the snap-through starting curvature. Hence, the snap-through moment is closely related to the cured curvature and the snap-through starting curvature.

First, in the case of snap-forth, the cured curvatures of Mode 1 (i.e., the starting deformation curvatures of the linear region of the $M_{x-1}\kappa_{xx}$ curve) increase linearly with the initial tool-plate curvature. However, the snap-forth starting curvatures (i.e., the ending deformation curvatures of the linear region of the $M_{x-1}\kappa_{xx}$ curve, which are indicated by the dots in Fig. 7(a)) are identical to each other regardless of the initial tool-plate curvature. For this reason, the difference between the cured curvature and the snap-forth starting curvature increases linearly with the initial tool-plate curvature. As a result, the snap-forth moment also increases linearly with increasing initial tool-plate curvature. The variation trend of the snap-forth moment with a change in the initial tool-plate curvature agrees well with the predicted result as presented earlier.

Additionally, the relation between the y-directional residual moment ${}_{Mode1}m_y^{Residual}$ and the snap-forth starting curvature supports the second assumption. As mentioned earlier, the y-directional residual-moment and the snap-forth starting curvature remain constant regardless of the initial tool-plate curvature. In other words, there is one-to-one correspondence between the y-directional residual moment and the snap-forth starting curvature, as expected earlier.

Second, in the case of snap-back, the cured curvatures of Mode 2 (i.e., the starting deformation curvatures of the linear region of the $M_{y-2}\kappa_{yy}$ curve) change very slightly with the initial tool-plate curvature. However, the snap-back starting curvatures (i.e., the ending deformation curvatures of the linear region of the $M_{y-2}\kappa_{yy}$ curve, which are indicated by the dots in Fig. 7(b)) decrease linearly with increasing initial tool-plate curvature. For this reason, the difference between the cured curvature and the snap-back starting curvature also decreases linearly with increasing initial

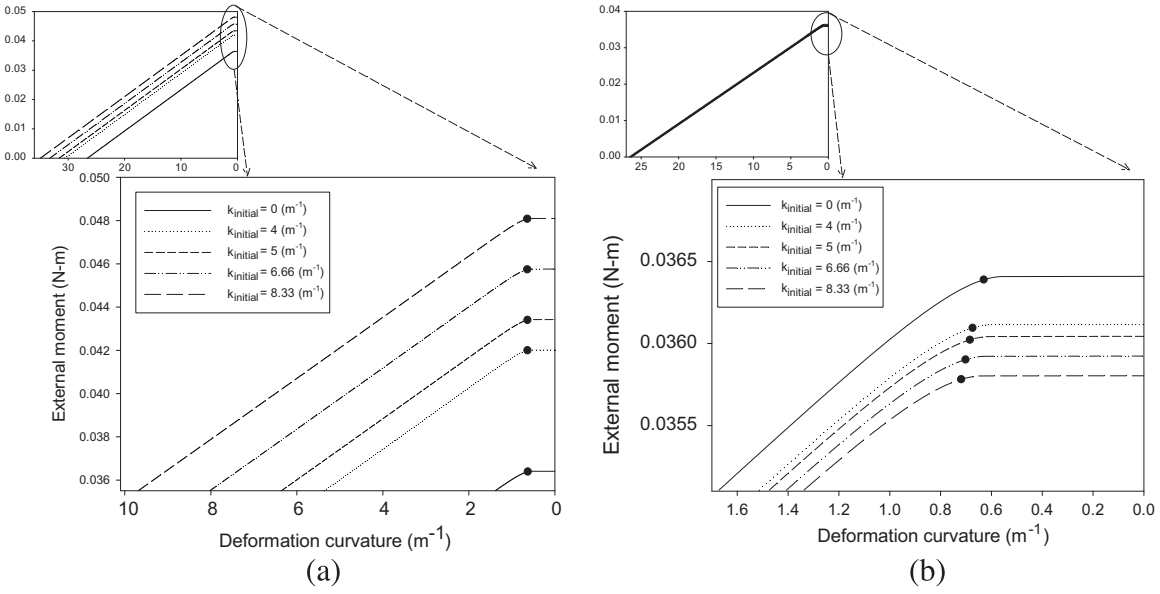

Fig. 7. Curve of moment vs. deformation curvature for each initial tool-plate curvature (analysis results): (a) snap-forth and (b) snap-back.

tool-plate curvature. As a result, the snap-back moment also decreases linearly with increasing initial tool-plate curvature. The variation trend of the snap-back moment with a change in the initial tool-plate curvature agrees well with the predicted result as presented earlier.

Additionally, the relation between the *x*-directional residual moment ${}_{Mode2}m_x^{Residual}$ and the snap-back starting curvature supports the second assumption. As mentioned earlier, the *x*-directional residual-moment and the snap-back starting curvature change with changing initial tool-plate curvature. Therefore, one-to-one correspondence also exists between the *x*-directional residual moment and the snap-back starting curvature. The interpretation of this result is that the increased residual moment makes it difficult to sustain a cylindrical shape with a relatively small curvature. For this reason, the snap-back of the bistable composite with an initial tool-plate curvature starts earlier than that of the bistable composite with a zero initial tool-plate curvature.

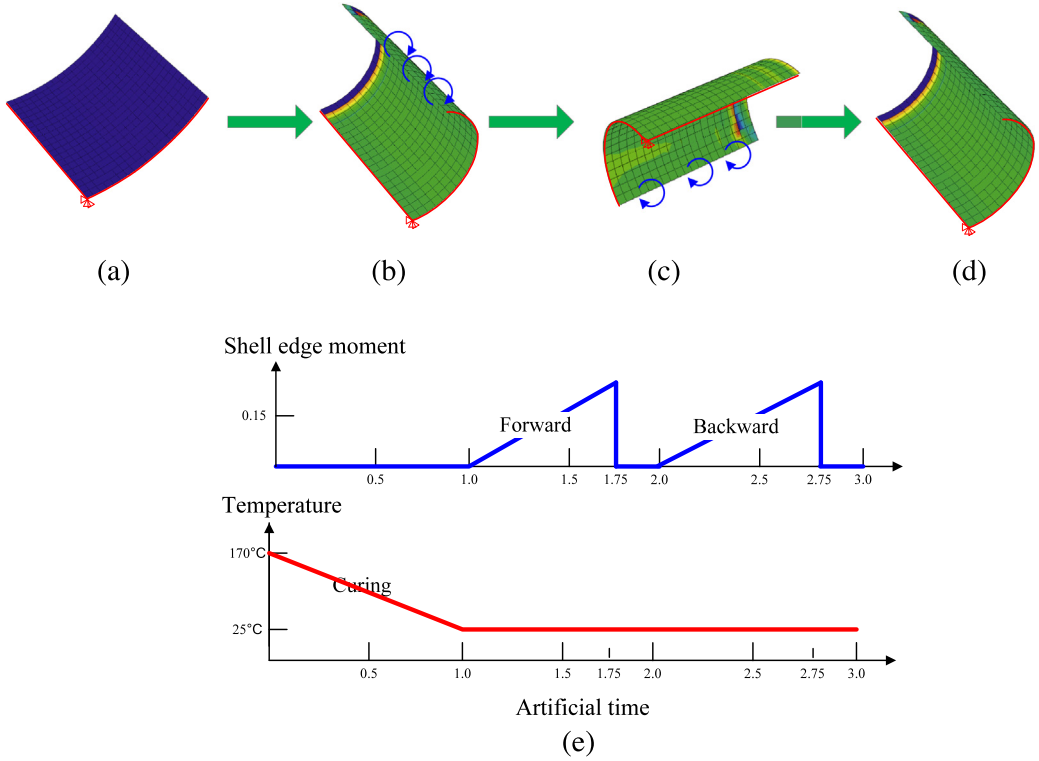

Fig. 8. FE analysis of snap-through of bistable composite subjected to a moment: (a) before curing process, (b) after curing process and snap-forth, (c) after snap-forth and snap-back, (d) after snap-back, and (e) loading history of FE analysis.

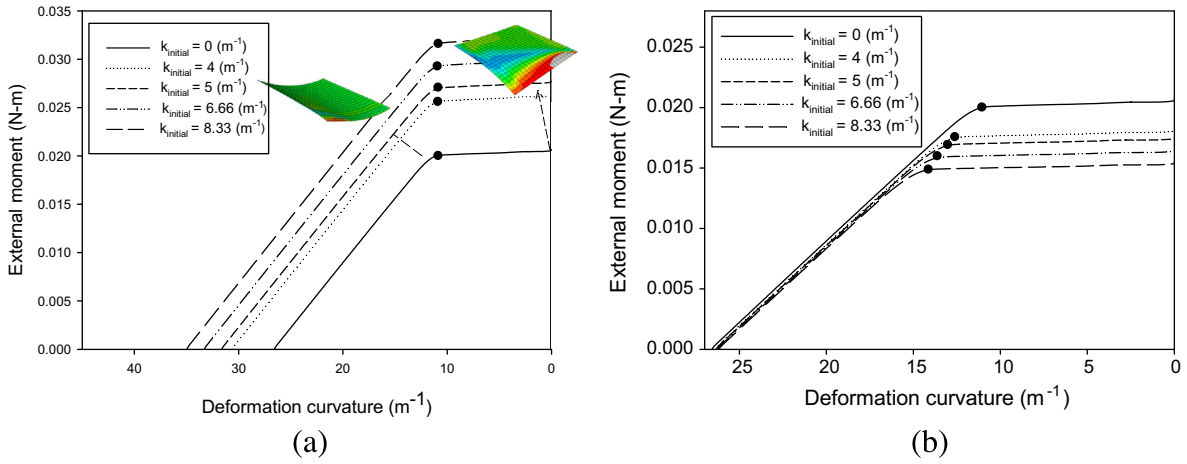

Fig. 9. Curve of moment vs. deformation curvature for each initial tool-plate curvature (FEA results): (a) $M_{x-1}\kappa_{xx}$ curve for snap-forth and (b) $M_{y-2}\kappa_{yy}$ curve for snap-back.

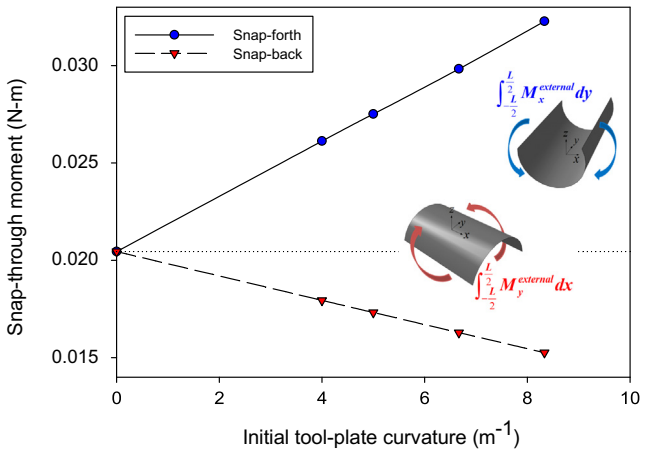

Fig. 10. Change in snap-through moment with initial tool-plate curvature (FEA results).

4. Verification of pre-identified effect of initial tool-plate curvature

4.1. FE analysis of snap-through moment of bistable composites

FE analysis was performed for obtaining results that are more accurate and for verifying the analysis results obtained by the present simple analytical model. Commercial FE software ABAQUS was used for the static analysis of the snap-though induced by an external moment [29]. The selected element was a four-node doubly curved thin shell element (S4). The mesh density was chosen as 20×20 elements in consideration of the convergence property and computation time. To reduce the computation time further, one quarter of the entire system was simulated on the basis of the symmetry of this problem [5].

The FE analysis was divided into two main processes—the curing process and the loading process—explained as follows.

1. In the curing process, the evaluated temperature (170 °C) is reduced to the service temperature (25 °C), as shown in

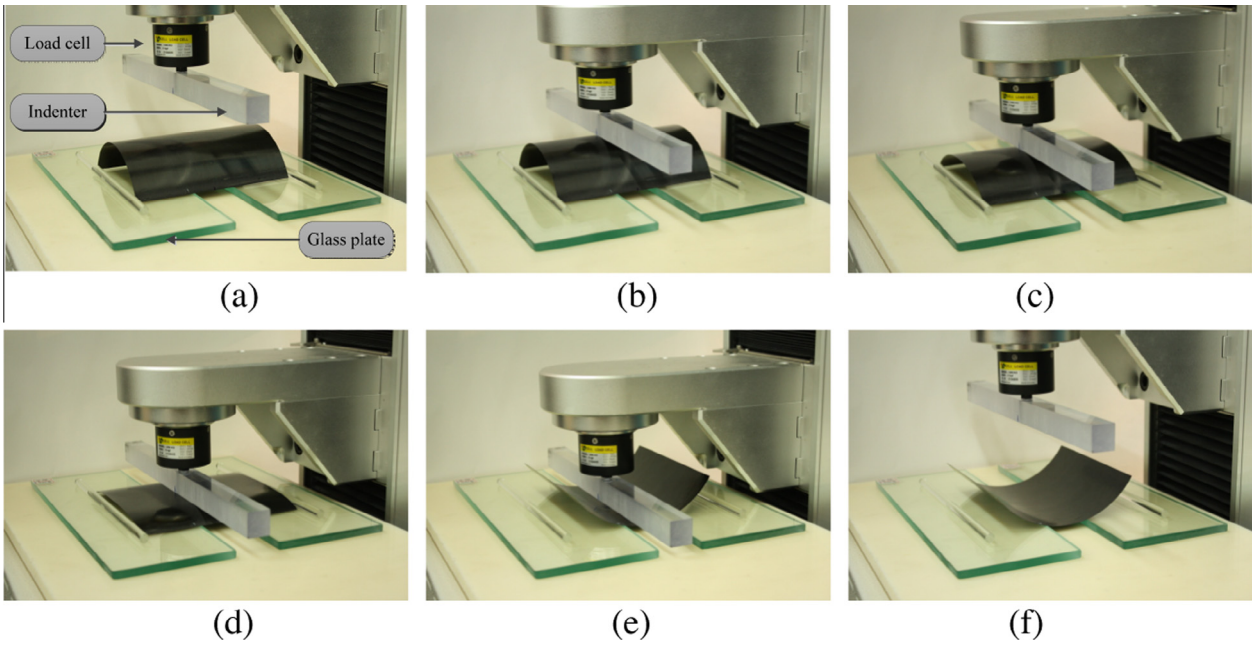

Fig. 11. Experimental procedure for measuring snap-through load: (a) setup for vertical load test, (b) load induced by surface-to-surface contact, (c) continuous pressing, (d), (e) snap-through, and (f) unloading after snap-through.

Fig. 8(e). Following the curing process, the bistable composite takes the cylindrical stable shape of Mode 1 or that of Mode 2, as illustrated in Fig. 8(b).

2. In the loading process, a moment is applied to the flat edge of the bistable composite to induce snap-through, as shown in Fig. 8(b).
   (1) During the loading process, the strain energy of the bistable composite increases with increasing moment. Snap-through eventually occurs at the maximum strain energy, the moment at which instant is taken as the snap-through moment in this case. After snap-through, the moment is removed to check the stability of the snapped cylindrical shape.
   (2) Following the relaxation, the moment is reapplied to the flat edge of the snapped bistable composites in the opposite direction to induce snap-through, as illustrated in Fig. 8(c). After snap-through has occurred, the corresponding moment is also removed.

As shown in Figs. 9 and 10, the results of the FE analysis demonstrate that the snap-forth moment and the snap-back moment respectively increase and decrease linearly with the initial tool-plate curvature, as was the trend in the pre-analysis. The magnitude of the overall snap-through moments in the FE analysis is smaller than those in the pre-analysis. Nonetheless, the effects of the initial tool-plate curvature on the snap-through moment are identical in both the FE analysis and the pre-analysis.

The difference between these two results is attributed to the assumption of a constant curvature in the analytical model. In the case of thin bistable composites, snap-through occurs under complex deformations (e.g., noncylindrical bending or warpage) [28]. However, this assumption cannot represent local complex warpage deformations. For this reason, the snap-through load in the analytical model is overestimated compared to the result obtained by three-dimensional FE analysis.

4.2. Experiment and FE analysis of snap-through vertical load of bistable composites

In the previously presented analyses in this paper, the effect of the initial tool-plate curvature on the snap-through moment was studied. In the practical experiment of this study, a vertical load

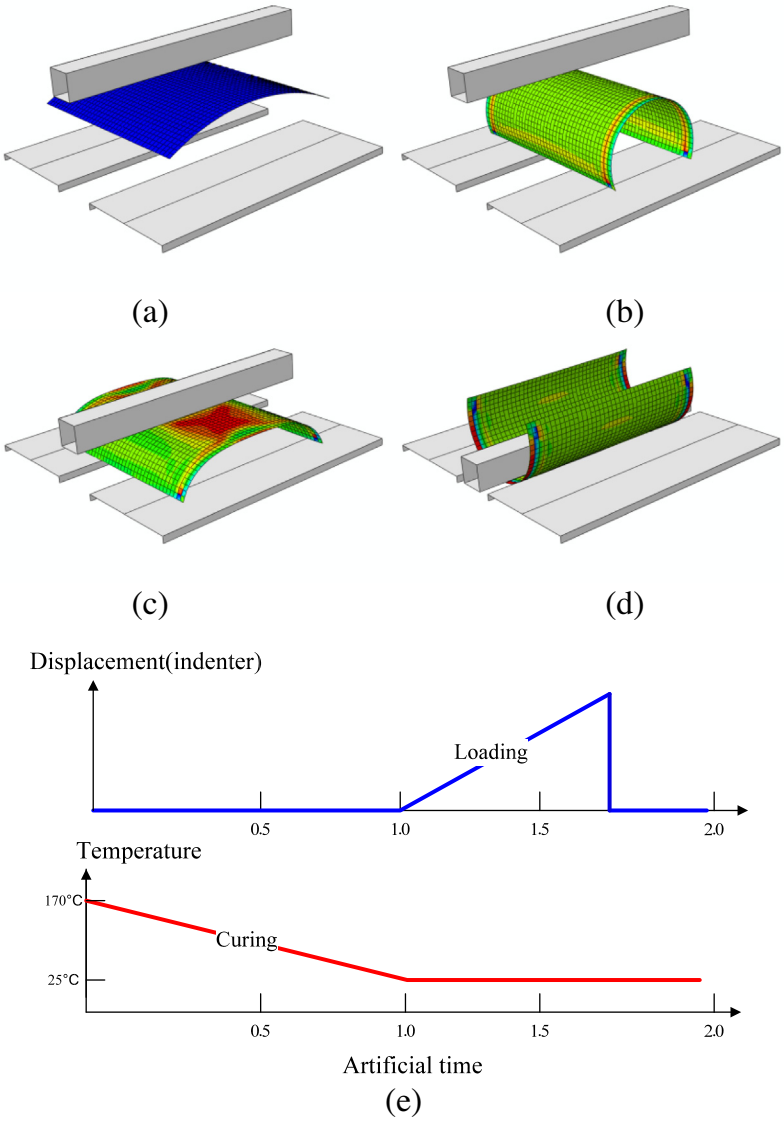

Fig. 12. FE analysis of snap-through of bistable composite subjected to line-pressing load: (a) before curing process, (b) after curing process, (c) deformation before snap-through, (d) after snap-through, and (e) loading history of FE analysis.

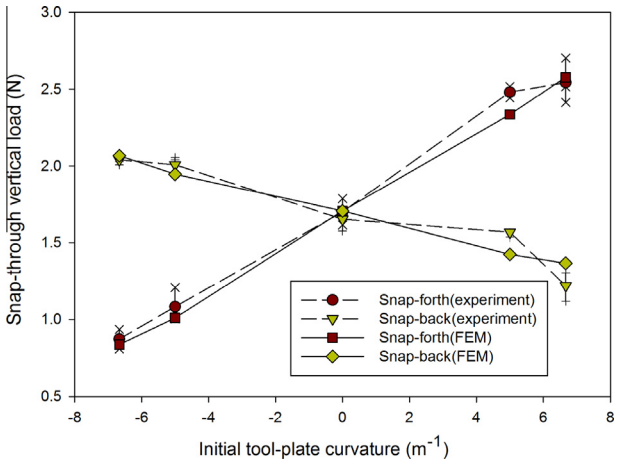

Fig. 13. Change in snap-through load with initial tool-plate curvature.

was considered instead of a distributed edge moment. Then, experiments and FE analysis were performed for evaluating the snap-through load of bistable composites subjected to a vertical load, where an experimentally realizable boundary condition was considered.

The experimental setup is shown in Fig. 11. An indenter is aligned parallel to the direction of the dominant curvature of the bistable composites. The indenter is fixed to the tensile machine. Therefore, the indenter is movable only in the vertical direction. The bistable composites are placed on two glass plates, which are lubricated by oil to minimize the friction between the edge of the bistable composites and the surface of the glass plate. The two glass plates are placed parallel to each other on the testing table at a constant distance. The distance is kept longer than the width of the indenter to prevent collision between the indenter and the glass plate.

Before the vertical load test, square cross-ply bistable composites with an initial curvature were manufactured. First, two laminae were cut into squares with a side length of 150 mm. The lamina with a 0° direction was placed on the tool plate, and its fiber was aligned in a direction parallel to the curvature direction of the tool plate. The lamina with a 90° direction was placed on the 0° direction lamina and its fiber was aligned in a direction perpendicular to the curvature direction of the tool plate. The cross-ply laminates were packaged in the same way as that done by Ryu et al. [27]. In the curing process, the temperature was elevated from room temperature (25 °C) to the curing temperature (170 °C). Then, the packaged laminates were cured in a curing oven for 2 h. The curing pressure was maintained at 1 atm by an external vacuum pump during the curing cycle.

The vertical load test was performed by the following procedure. First, the indenter and the bistable composites were separated from each other as shown in Fig. 11(a). As the indenter moved downward, its bottom surface came into contact with the top surface of the bistable composites, as shown in Fig. 11(b). At this instant, the vertical load was induced by surface-to-surface contact; following this, the deformation of the bistable composites was initiated (Fig. 11(c) and (d)). The vertical load was applied quasi-statically with downward motion of the indenter until snap-through occurred. The vertical load at which snap-through occurs is defined as the snap-through vertical load.

The FE analysis was performed in the same way as the vertical load test. The FE models used for FE analysis consisted of the bistable composites, a rigid indenter, and a rigid plate part, as illustrated in Fig. 12. The four-node doubly curved thin shell element (S4) was selected for the simulation of the snap-through of the bistable composites. The mesh density for the bistable composites was chosen as 1600 elements. In order to minimize mesh dependency of the snap-through vertical load, the analytical rigid surface in ABAQUS [20], which does not require meshes, was employed for generating the rigid components except for the bi-stable composites (i.e., the rigid indenter and the rigid plate part).

4.3. Comparison between experimental and FEA results

For the snap-through experiments, five different initial tool-plate curvatures—0, ±5, and ±6.667 m^{-1}—were considered. For each of these initial curvatures, three bistable composite specimens were manufactured. The vertical load tests were performed six times for each bistable composite specimen: three times for snap-forth and three times for snap-back.

From the experimental and FEA results presented in Fig. 13, we found that the snap-through vertical loads were proportional to the initial tool-plate curvatures. As shown in Fig. 10, the line moment acting on the square cross-ply bistable composite specimens also showed this linearity with the value of the initial tool-plate curvature. Further, as shown in Fig. 13, the snap-through vertical load obtained by FE analysis was in excellent agreement with that obtained experimentally.

5. Conclusion

In this study, the snap-through of square cross-ply bistable composites was simulated and experimentally validated in order to evaluate the effect of the initial tool-plate curvature on the snap-through load. This effect was estimated by the present simple analytical model. Furthermore, for the validation of the pre-identified initial tool-plate curvature effect, experiments and FE analysis were performed under a practical loading condition (i.e., vertical load). The following conclusions were drawn from these analyses.

1. The snap-forth load increases linearly with increasing initial tool-plate curvature.
2. In contrast, the snap-back load decreases linearly with increasing initial tool-plate curvature.

Given this linear relation, the snap-through load of square cross-ply bistable composites with an arbitrary initial curvature can be easily predicted by just two snap-through experiments: with and without the initial curvature. Additionally, the approach of adding an initial curvature is expected to reduce the design complexity of square cross-ply bistable composites because the snap-through load is controllable without any changes in the existing design variables (e.g., thickness and lay-up sequence). For all these reasons, we expect that the designers of bistable composites will be able to easily predict and design the snap-through load by making use of the initial tool-plate curvature effect through a simple analysis.

Acknowledgements

This work was supported by the National Research Foundation of Korea (NRF) Grant funded by the Korea government (MSIP) (No. 2012R1A3A2048841).

References

[1] Hyer MW. Some observation on the cured shape of thin unsymmetric laminates. J Compos Mater 1981;15:175–94.
[2] Hyer MW. The room-temperature shapes of four-layer unsymmetric cross-ply laminates. J Compos Mater 1982;16:318–40.

[3] Jun WJ, Hong CS. Effect of residual shear strain on the cured shape of unsymmetric cross-ply thin laminates. Compos Sci Technol 1990;38:55–67.
[4] Jun WJ, Hong CS. Cured shape of unsymmetric laminates with arbitrary lay-up angles. J Reinf Plast Compos 1992;11:1352–66.
[5] Ren L, Parvizi-Majidi A, Li Z. Cured shape of cross-ply composite thin shells. J Compos Mater 2003;37:1801–20.
[6] Cho M, Kim MH, Choi HS, Chung CH, Ahn KJ, Eom YS. A study on the room-temperature curvature shapes of unsymmetric laminates including slippage effects. J Compos Mater 1998;32:460–82.
[7] Cho M, Roh H. Non-linear analysis of the curved shape of unsymmetric laminates accounting for slippage effects. Compos Sci Technol 2003;63:2265–75.
[8] Lee J-G, Ryu J, Lee H, Cho M. Saddle-shaped bi-stable morphing panel with shape memory alloy spring actuator. Smart Mater Struct 2014;23:0740133.
[9] Dano ML, Hyer MW. Snap-through of unsymmetric fiber-reinforced composite laminates. Int J Solids Struct 2002;39:175–98.
[10] Dano ML, Hyer MW. SMA-induced snap-through of unsymmetric fiber-reinforced composite laminates. Int J Solids Struct 2003;22:5949–72.
[11] Diaconu CG, Weaver PM, Arrieta AF. Dynamic analysis of bi-stable composite plates. J Sound Vib 2009;322:987–1004.
[12] Mattioni F, Weaver PM, Friswell MI, Potter KD. Modelling and applications of thermally induced multistable composites with piecewise variation of lay-up in the planform. In: 48th AIAA/ASME/ASCE/AHS/ASC structures, structural dynamics and materials conference AIAA. Honolulu, Hawaii; April, 2007.
[13] Schultz MR. A concept for airfoil-like active bistable twisting structures. J Intell Mater Syst Struct 2008;19:157–69.
[14] Daynes S, Potter KD, Weaver PM. Aeroelastic study of bistable composite airfoils. J Aircr 2009;46:2169–73.
[15] Arrieta AF, Bilgen O, Friswell MI, Hagedorn P. Passive load alleviation bi-stable morphing concept. AIP Adv 2012;2:032118.
[16] Arrieta AF, Kuder IK, Rist M, Weaber T, Ermanni P. Passive load alleviation aerofoil concept with variable stiffness multi-stable composites. Bi-stable morphing concept. Compos Struct 2014;116:235–42.
[17] Pirrera A, Avitabile D, Weaver PM. Bistable plate for morphing structure: a refined analytical approach. Int J Solids Struct 2010;47:3412–25.
[18] Arrieta AF, Bilgen O, Friswell MI, Ermanni P. Modelling and configuration control of wing-shaped bi-stable piezoelectric composites under aerodynamic loads. Aerosp Sci Technol 2013;29:453–61.
[19] Arrieta AF, Hagedorn P, Erturk A, Inman DJ. A piezoelectric bistable plate for nonlinear broadband energy harvesting. Appl Phys Lett 2010;97:104102.
[20] Betts DN, Kim HA, Bowen CR, Inman DJ. Optimal configuration of bistable piezo-composites for energy harvesting. Appl Phys Lett 2012;100:114104.
[21] Kim S-W, Koh J-S, Lee J-G, Ryu J, Cho M, Cho K-J. Flytrap-inspired robot using structurally integrated actuation based on bistability and developable surface. Bioinspiration Biomimetics 2014;9:036004.
[22] Panesar AS, Weaver PM. Optimisation of blended bistable laminates for a morphing flap. Compos Struct 2012;94:3092–105.
[23] Sousa CS, Camanho PP, Suleman A. Analysis of multistable variable stiffness composite plates. Compos Struct 2013;98:34–46.
[24] Arrieta AF, Kuder IK, Waeber T, Ermanni P. Variable stiffness characteristics of embeddable multi-stable composites. Compos Sci Technol 2014;97:12–8.
[25] Daynes S, Potter KD, Weaver PM. Bistable prestressed buckled laminates. Compos Sci Technol 2008;68:3431–7.
[26] Daynes S, Diaconu CG, Potter KD, Weaver PM. Bistable prestressed symmetric laminates. J Compos Mater 2010;44:1119–37.
[27] Ryu J, Kong J-P, Kim S-W, Cho K-J, Cho M. Curvature tailoring of unsymmetric laminates with an initial curvature. J Compos Mater 2013;47:3163–74.
[28] Potter K, Weaver P, Seman AA, Shah S. Phenomena in the bifurcation of unsymmetric composite plates. Compos: Part A 2007;38:100–6.
[29] ABAQUS/CAE Version 6.12; 2012.